



HAL
open science

Two temperate corals are tolerant to low pH regardless of previous exposure to natural CO₂ vents

Chloe Carbonne, Núria Teixidó, Billy Moore, Alice Mirasole, Thomas Guttierrez, Jean-Pierre Gattuso, Steeve Comeau

► To cite this version:

Chloe Carbonne, Núria Teixidó, Billy Moore, Alice Mirasole, Thomas Guttierrez, et al.. Two temperate corals are tolerant to low pH regardless of previous exposure to natural CO₂ vents. *Limnology and Oceanography*, In press, 66 (11), pp.4046-4061. 10.1002/lno.11942 . hal-03348884

HAL Id: hal-03348884

<https://hal.science/hal-03348884>

Submitted on 20 Sep 2021

HAL is a multi-disciplinary open access archive for the deposit and dissemination of scientific research documents, whether they are published or not. The documents may come from teaching and research institutions in France or abroad, or from public or private research centers.

L'archive ouverte pluridisciplinaire **HAL**, est destinée au dépôt et à la diffusion de documents scientifiques de niveau recherche, publiés ou non, émanant des établissements d'enseignement et de recherche français ou étrangers, des laboratoires publics ou privés.

1 **Two temperate corals are tolerant to low pH regardless of**
2 **previous exposure to natural CO₂ vents**

3 Chloe Carbonne^{1,*}, Nuria Teixidó^{1,2}, Billy Moore^{1,3}, Alice Mirasole², Thomas

4 Gutierrez^{1,4}, Jean-Pierre Gattuso^{1,5}, Steeve Comeau¹

5 ¹ Sorbonne Université, CNRS, Laboratoire d'Océanographie de Villefranche, 181 chemin du Lazaret,
6 06230 Villefranche-sur-mer, France

7 ² Stazione Zoologica Anton Dohrn, Ischia Marine Centre, Department of Integrated Marine Ecology,
8 Punta San Pietro, 80077, Ischia (Naples), Italy

9 ³ MSc Tropical Marine Biology, University of Essex, Wivenhoe Park, Colchester CO4 3SQ, United
10 Kingdom

11 ⁴ Master Science de la Mer, Aix-Marseille Université, 58 bd Charles Livon, 13284 Marseille Cedex
12 07, France

13 ⁵ Institute for Sustainable Development and International Relations, Sciences Po, 27 rue Saint
14 Guillaume, F-75007 Paris, France

15 *Corresponding author: chloe.carbonne@imev-mer.fr

16 Running head: Coral tolerance to ocean acidification

17 Keywords: ocean acidification, CO₂ vents, temperate, Mediterranean, coral, *Cladocora*
18 *caespitosa*, *Astroides calycularis*, calcification, tolerance, low pH

19

20

21

22

23

24 **Abstract**

25 Ocean acidification is perceived to be a major threat for many calcifying organisms, including
26 scleractinian corals. Here we investigate (1) whether past exposure to low pH environments
27 associated with CO₂ vents could increase corals tolerance to low pH and (2) whether
28 zooxanthellate corals are more tolerant to low pH than azooxanthellate corals. To test these
29 hypotheses, two Mediterranean colonial corals *Cladocora caespitosa* (zooxanthellate) and
30 *Astroides calycularis* (azooxanthellate) were collected from CO₂ vents and reference sites and
31 incubated in the laboratory under present-day (pH on the total scale, pH_T 8.07) and low pH
32 conditions (pH_T 7.70). Rates of net calcification, dark respiration and photosynthesis were
33 monitored during a six-month experiment. Monthly net calcification was assessed every 27 to
34 35 d using the buoyant weight technique, whereas light and dark net calcification was
35 estimated using the alkalinity anomaly technique during 1 h incubations. Neither species
36 showed any change in net calcification rates, respiration, and photosynthesis regardless of
37 their environmental history, pH treatment and trophic strategy. Our results indicate that *C.*
38 *caespitosa* and *A. calycularis* could tolerate future ocean acidification conditions for at least 6
39 months. These results will aid in predicting species' future responses to ocean acidification,
40 and thus improve the management and conservation of Mediterranean corals.

41

42

43

44

45

46

47

48 **Introduction**

49 Ocean acidification describes the shift in carbonate chemistry caused by the uptake of
50 anthropogenic CO₂ by the ocean (Caldeira and Wickett 2003, Gruber et al. 2019). It causes an
51 increase in dissolved inorganic carbon and bicarbonate ion concentrations, along with a
52 concurrent decrease in pH, carbonate ion concentration and its associated saturation state (Ω ;
53 Orr et al. 2005). Calcifying species are perceived to be particularly vulnerable to ocean
54 acidification (Kroeker et al. 2013a). For example, corals are particularly sensitive to changes
55 in carbonate chemistry as their skeleton is made of aragonite, a metastable form of calcium
56 carbonate that is less stable than calcite (Erez et al. 2011, Foster and Clode 2016). As a result,
57 coral calcification is expected to decrease as seawater acidity increases (Gattuso et al. 1999).
58 Coral calcification decreases by on average 22% under pH values expected by the end of the
59 century under the high-CO₂ emissions scenario (RCP 8.5 from AR5 of ICPP; Chan and
60 Connolly 2013). However, a range of contradictory species- and experience-specific
61 responses have been described (e.g. Kornder et al. 2018), with some species such as massive
62 *Porites* spp. being tolerant to ocean acidification (Fabricius et al. 2011). This resistance to
63 ocean acidification was also described in several temperate and cold-water corals (e.g.
64 Rodolfo-Metalpa et al. 2010). Such tolerance is seen in many studied parameters such as net
65 calcification rate, respiration, photosynthetic physiology, calcifying fluid pH (McCulloch et
66 al. 2012a, Wang et al. 2020). According to Varnerin et al. (2020) even juveniles from the
67 temperate *Oculina arbuscula* were only slightly affected by ocean acidification.

68 A central question when assessing the future of corals in a high-CO₂ world is whether they
69 have the capacity to acclimatize and further adapt to ocean acidification. This question
70 remains unanswered as corals are generally long-lived organisms for which it is extremely
71 challenging to study acclimatization and adaptation processes over several generations.

72 Acclimatization refers to reversible phenotypic changes limited by genotype, occurring under

73 naturally varying conditions by a physiological readjustment of the organism's tolerance
74 levels (Edmunds and Gates 2008). In contrast, adaptation refers to changes in the genetic
75 composition of a population by natural selection, in which traits will be passed on to the next
76 generation (Savolainen et al. 2013). In a recent study, Cornwall et al. (2020) conducted a one-
77 year experiment showing that coralline algae have the capacity to acclimatize to low pH after
78 seven generations of exposure. Replicating such a study on corals is virtually impossible as
79 they are long-lived organisms which only reach sexual maturity after several years. CO₂ vents
80 therefore offer a unique opportunity to investigate the response of corals to ocean acidification
81 over long periods of time. In such systems, volcanic CO₂ bubbles from the seafloor which
82 acidifies the surrounding seawater and creates an environment, with carbonate chemistry
83 conditions that mimic those expected in the future (Hall-Spencer et al., 2008, Camp et al.
84 2018, González-Delgado and Hernández 2018). By investigating individuals, species, and
85 communities along transects radiating from the sources of CO₂, it is possible to substitute time
86 for space. It must be pointed out, however, that CO₂ vents are imperfect windows into the
87 future because they generally do not mimic other climate-related changes such as ocean
88 warming. Furthermore, it is not possible to disentangle any changes in the mean versus
89 variability of seawater pH (Hall-Spencer et al. 2008). Overall, these systems exhibit
90 significant decreases in trophic complexity and biodiversity, as well as a major decrease in the
91 abundance of calcifying organisms (Kroeker et al. 2013b, Linares et al. 2015, Teixidó et al.
92 2018). Corals living in the vicinity of CO₂ vents have been exposed to low and high
93 variability pH conditions for an extended period of time (years to decades). They are therefore
94 ideal models to investigate acclimatization and adaptation to ocean acidification (Fantazzini et
95 al. 2015, Foo et al. 2018). Populations or individuals living in these variable and more
96 extreme environments are hypothesized to be more tolerant to suboptimal environmental
97 conditions such as acidification (e.g. Cornwall et al. 2018).

98 CO₂ vents have been used for transplant experiments between acidified and nearby reference
99 sites with ambient pH and no vent activity. For example, a decline in calcification was
100 described in the zooxanthellate corals *Cladocora caespitosa* and *Balanophyllia europaea*
101 transplanted to a CO₂ vent site in Ischia (Rodolfo-Metalpa et al. 2011). The skeletal growth of
102 *Porites astreoides* living in a natural pH gradient showed no acclimatization to ocean
103 acidification despite their life-long exposure to low pH (Crook et al. 2013). Few laboratory
104 studies have focused on temperate scleractinian corals from natural CO₂ vents despite the
105 relevance of studying the tolerance of temperate coral populations to ocean acidification
106 (Trotter et al. 2011, Teixidó et al. 2020). Such studies are important for understanding and
107 elucidating how these species will respond to the suboptimal pH conditions projected for the
108 end of this century.

109 The symbiosis between scleractinian corals and endosymbiotic algae, commonly referred to
110 as zooxanthellae, has been studied thoroughly (Davy et al. 2012). Photosynthetic products
111 from zooxanthellae contribute significantly to the energy budget of the scleractinian host
112 (Allemand et al. 2011, Muller-Parker et al. 2015) and can play an important role in
113 calcification (Erez et al. 2011, Inoue et al. 2018). However, not all corals harbor
114 zooxanthellae (azooxanthellate corals). Gibbin et al. (2014) demonstrated that zooxanthellae
115 regulate intracellular pH under acidified conditions, whereas azooxanthellate corals can suffer
116 from reduced intracellular pH which can lead to intracellular acidosis. It can thus be expected
117 that photosynthesis may enhance calcification by (1) providing energy for this energetically
118 costly process and (2) by increasing pH at the site of calcification (Allemand et al. 2011). In a
119 transplant experiment in the CO₂ vents of Panarea, Prada et al. (2017) showed that the
120 calcification of two azooxanthellate corals *Leptopsammia pruvoti* and *Astroides calycularis*
121 decreased at low pH, whereas calcification of the zooxanthellate coral *B. europaea* was
122 unaffected. A similar result was observed in pH-controlled aquaria by Ohki et al. (2013) as

123 polyps of *Acropora digitifera* with symbionts showed higher calcification rates than polyps
124 without symbionts under low pH, suggesting that symbionts confer tolerance to ocean
125 acidification. However, in a study led by McCulloch et al. (2012b), azooxanthellate cold-
126 water corals presented higher intracellular pH regulation than shallow-water zooxanthellate
127 corals under acidification. As it is not truly known whether or not symbionts promote the
128 maintenance of elevated pH at the site of calcification, it is interesting to compare
129 zooxanthellate and azooxanthellate corals as they may display contrasting responses to ocean
130 acidification.

131 The present study focuses on two Mediterranean long-lived corals of key relevance for
132 conservation, the zooxanthellate species *C. caespitosa* (Linnaeus, 1767) and the
133 azooxanthellate species *A. calycularis* (Pallas, 1766). *Cladocora caespitosa* is a unique
134 zooxanthellate reef-building coral that provides a valuable ecosystem service in the
135 Mediterranean Sea which is lacking large bioconstructions (Kersting and Linares 2012).
136 *Astroides calycularis* is commonly found in the southwestern Mediterranean Sea and can be
137 highly abundant in low light, shallow rocky habitats (Zibrowius 1995). These two
138 scleractinian corals naturally occur at two newly discovered CO₂ vent systems along the coast
139 of Ischia, Italy. In situ data obtained by Teixidó et al. (2020) showed variable responses in
140 skeletal structure and growth patterns of *A. calycularis*, with colonies from the CO₂ vent site
141 characterized by smaller size, fewer polyps, and less porous, denser skeletons. Thus, these
142 two scleractinian coral species grown under elevated pCO₂ environments are great model
143 systems for assessing tolerance to acidification. Here, two hypotheses are tested: (1) past
144 exposure to low pH conditions confers tolerance to ocean acidification and (2) the coral-algal
145 symbiosis modulates this tolerance. To test these hypotheses, corals from natural CO₂ vent
146 systems and reference sites were exposed to present-day (pH on the total scale, pH_T ~ 8.07)

147 and low pH conditions ($\text{pH}_T \sim 7.70$) during a six-month long laboratory experiment, in which
148 calcification, respiration and photosynthesis rates were assessed.

149 **Material and Methods**

150 Study sites

151 We studied populations of the corals *Cladocora caespitosa* and *Astroides calycularis* that
152 naturally occur at two distinct CO_2 vent sites with low pH, and two reference sites with
153 ambient pH and no vent activity at the island of Ischia, Italy (Fig. S1 Supplementary
154 materials). *Cladocora caespitosa* occurs near a CO_2 vent site adjacent to rocky reefs at about
155 10 m depth (Chiane del Lume, hereafter Vent 1), whereas *A. calycularis* occurs in another
156 CO_2 vent site between 1 - 2 m depth (Grotta del Mago, a semi-submerged cave hereafter Vent
157 2, where CO_2 vents occur at 5 m depth). Vent gas compositions at Vent 1 and Vent 2 were
158 predominantly CO_2 (mean \pm SE: 93.9 ± 0.6 for Vent 1, 93.4 ± 1.0 for Vent 2), with
159 undetectable levels of hydrogen sulfide (< 0.0002 %), and did not elevate the temperature (for
160 more information on gas measurements, see Teixidó et al. 2020). The reference sites without
161 any visible vent activity and exhibiting ambient pH were located: i) approximately 100 m
162 west from Vent 1 for *C.caespitosa* (hereafter Ambient 1, 10 m depth) and ii) 1.5 km away
163 from Vent 2 for *A. calycularis* (San Pancrazio, an overhang, hereafter Ambient 2, 1-2 m
164 depth) (Fig. S1 Supplementary materials).

165 Coral field surveys

166 The *C. caespitosa* abundance was quantified using 12 quadrats of 50 cm x 50 cm, which were
167 randomly placed along the rocky reef at 10 m depth at the two sites ($n = 24$ quadrats in total).
168 Abundance was assessed by counting the number of colonies found in each quadrat. In
169 addition, size of colonies was determined by measuring the major colony diameter with a

170 plastic ruler (with an error of ± 1 cm) (Peirano et al. 2001). Major colony diameter was
171 selected as the best colony size descriptor (Kersting 2012). The *A. calycularis* abundance was
172 quantified using 12 photo-quadrats (25 x 25 cm) between 1 and 2 m depth in the two other
173 sites ($n = 24$ quadrats in total, Vent 2, Ambient 2). Size frequency-distribution was calculated
174 by counting the number of polyps of each colony and each colony was then pooled into one of
175 five size classes (I: 1-5 polyps; II: 6-10 polyps; III: 11-15 polyps; IV: 16-20 polyps; V: > 20
176 polyps). The survey's depth for *C. caespitosa* and *A. calycularis* corresponded to the depth
177 range at which colonies were sampled for the experiment (see below). Abundance and size-
178 frequency data for *A. calycularis* have been described previously in Teixidó et al. (2020).

179 In situ pH_T and carbonate chemistry associated with CO₂ vents and ambient pH sites

180 SeaFETTM Ocean pH sensors (Satlantic) were deployed to quantify variation in pH at the two
181 CO₂ vent and the two ambient pH sites. Measurements were taken every 15 minutes. One sensor
182 was deployed at the Vent 1 site from May 7 to 21, 2019, and one sensor was deployed at the
183 Ambient 1 site during the same period. At the semi-submerged cave (Vent 2), sensors were
184 deployed in May-June 2019 (before summer) and in September 2018 (after summer). Dates of
185 deployment for Vent 2 were from September 8 to September 24, 2018 and from May 30 to June
186 18, 2019 at Vent 2. One sensor was deployed in the reference area Ambient 2 during the same
187 period. Before deployment, the SeaFETs were calibrated with ambient pH water in the
188 aquarium facilities at the Center Villa Dohrn (Ischia, Italy). The mean offset between
189 calibration samples and calibrated SeaFET pH was ± 0.002 units, indicating high quality pH
190 dataset. Discrete water samples were collected using Niskin bottles to measure the carbonate
191 system parameters during the pH sensor deployment. Samples for total alkalinity (A_T) were
192 collected using standard operating protocols. The HCl (0.1 M) titrant solution was calibrated
193 against certified reference materials distributed by A.G. Dickson (CRM, Batches #153, #171,
194 and #177). Precision of the A_T measurements of CRMs was < 2 and $< 1 \mu\text{mol kg}^{-1}$ from nominal

195 values. A_T and pH_T were used to determine the remaining carbonate system parameters at in
196 situ temperature and depth of each sampling period in the R package seacarb v3.2.12. For full
197 details of pH sensors deployment, calibration, and total alkalinity standard operating protocols,
198 see Teixidó et al. (2020).

199 Coral collection

200 A total of 81 colonies of *C. caespitosa* and *A. calycularis* were randomly sampled for the
201 aquarium experiment. Fourteen (Vent 1) and sixteen (Ambient 1) colonies of *C. caespitosa*
202 were collected at 10 m depth; twenty-seven (Vent 2) and fourteen (Ambient 2) colonies of *A.*
203 *calycularis* were collected from 1 to 2 m depth. A portion of approximately 3 x 3 cm was
204 gently dislodged from each colony using a hammer and chisel. They were placed in coolers
205 filled with seawater changed regularly and maintained in Ischia for two days prior to
206 transportation to the aquarium facilities of the *Laboratoire d'Océanographie de Villefranche*,
207 France. The duration of the transfer was less than 10 h; colonies were wrapped in seawater-
208 soaked paper tissues. The colonies were cleaned, tagged with a number stuck under it using
209 water-resistant epoxy glue, and maintained at an ambient pH_T of ~8.05 during 2 weeks.

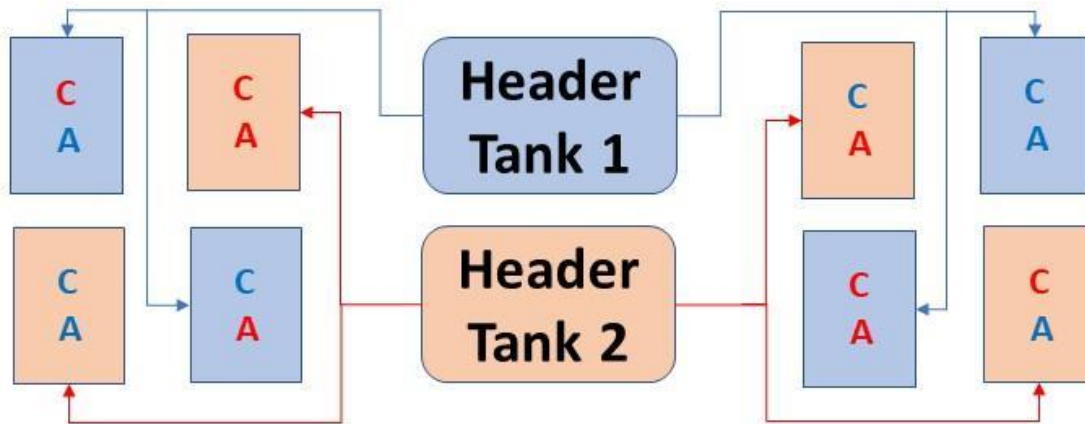
210 Experimental set-up and treatments

211 Colonies of *C. caespitosa* and *A. calycularis* were maintained in two constant pH treatments
212 during six months (202 days), one “present-day” treatment with a $pH_T = 8.08 \pm 0.01$ (mean \pm
213 SE, $n = 348$, total number of weekly pH_T measures in each 12 present-day experimental tank)
214 and one “low pH” treatment with a $pH_T = 7.72 \pm 0.01$ (mean \pm SE, $n = 348$, total number of
215 weekly pH_T measures in each 12 low pH experimental tank) corresponding to the pH values
216 expected by the end of the century under the RCP 8.5 CO₂ emissions scenario. More
217 specifically, 14 colonies from Vent 1 and 16 colonies from Ambient 1 of *C. caespitosa* and 27
218 from Vent 2 and 14 from Ambient 2 of *A. calycularis* were used for this experiment. The vent-

219 low pH condition was used to test the acclimation or long-term tolerance of the colonies to
220 low pH in the lab, after a life-time of exposure to in situ low pH. The ambient-low pH
221 condition was used to test the short-term tolerance to low pH of colonies that have not been
222 exposed to low pH before. The vent-present day condition tested the response to ambient pH
223 of colonies exposed in the long-term to in situ low pH. The ambient-present day condition
224 was the control. There were six independent 5 L experimental tanks for each of the four
225 conditions (origin x pH treatment), for a total of 24 experimental tanks. Each experimental
226 tank contained one to three colonies of each species, depending on their size, to get
227 approximately the same total amount of polyps per tank (Tab. S1 Supplementary materials).
228 Seawater pumped from Villefranche Bay at 5 m depth was continuously flowing into six 25 L
229 header tanks, used as water storage and to maintain gravity pressure for water flow into the
230 experimental tanks. Three header tanks were maintained at $\text{pH}_T \sim 8.07$ (present-day
231 treatment) and the other three at $\text{pH}_T \sim 7.7$ (low pH treatment). pH was controlled in the
232 header tanks using pH controllers (APEX, Neptune Systems) which regulated the delivery of
233 pure CO_2 . Each header tank gravity-fed four experimental four-liter tanks at a rate of 100 ml
234 min^{-1} (Fig. 1).

235 Light was provided by 89 W LED light bars (Aquadistik, Aqualumix). Irradiance gradually
236 increased from 0 at 06:00 to a maximum irradiance of $180 \mu\text{mol photons m}^{-2} \text{ s}^{-1}$ between
237 11:00 and 14:00, and gradually decreased to 0 at 18:00. According to the attenuation
238 coefficients of PAR in Villefranche Bay calculated in Martin and Gattuso (2009), the
239 maximum irradiance levels used in the study ($180 \mu\text{mol photons m}^{-2} \text{ s}^{-1}$) is within the
240 irradiance range observed at 10 m, where *Cladocora caespitosa* can be found in the
241 Mediterranean Sea (154 to $449 \mu\text{mol photons m}^{-2} \text{ s}^{-1}$). As *A. calycularis* were collected in a
242 semi-submerged cave and an overhang, dark plastic bags covered one side of the experimental
243 tanks to shade colonies from direct light. The 24 experimental tanks were kept in 6 water

244 baths under controlled temperature following Ischia's natural changes (Fig. S2 Supplementary
 245 materials, APEX, Neptune Systems). Submersible pumps (NEWA) provided water motion in
 246 each experimental tank. Three times a week, each tank was provided with a 30 mL solution of
 247 freshly hatched brine shrimps (*Artemia* sp.) for feeding.



x 3 replicates

<u>pH treatment</u>	<u>Origin</u>	<u>Species</u>
 Present day	Ambient	C <i>Cladocora caespitosa</i>
 Low pH	Vent	A <i>Astroides calycularis</i>

248 **Figure 1. Experimental set-up used to test the effects of origin (ambient vs vent site) and**
 249 **pH treatment (present day, $pH_T = 8.07 \pm 0.01$ and low pH, $pH_T = 7.72 \pm 0.01$) on the**
 250 **coral *C. caespitosa* and *A. calycularis*.** The experimental set-up was repeated 3 times,
 251 resulting in 6 header tanks, and 24 experimental tanks in which corals were randomly
 252 assigned.

253 Health status of experimental colonies

254 With pictures at the start of the experiment, each colony has been classified into two
 255 categories: colonies with loss of coenosarc (tissue between polyps) and colonies with tissue
 256 connecting their polyps. The number of dead polyps per colony (complete disappearance of
 257 tissue in the calice) was counted by comparing the pictures of the same colony at the start and
 258 the end of the experiment.

259 Carbonate chemistry in experimental tanks

260 pH in the header and experimental tanks was measured weekly using a handheld pH-meter
261 (826 pH mobile, Metrohm) calibrated with a TRIS buffer (batch #T33 provided by A.
262 Dickson, Scripps Institution of Oceanography, USA) before each set of measurements. Total
263 alkalinity (A_T) of each experimental and header tank was measured weekly during the first
264 four weeks in order to ascertain whether conditions were altered by metabolic activity.
265 Subsequently, and for the remainder of the experiment, A_T was measured every month in four
266 randomly selected tanks and one header. A_T was determined by potentiometric titration using
267 a Metrohm 888 Titrande following the method of (Dickson et al. 2007). Titrations of certified
268 reference material (Batch #186) provided by A. Dickson were used to assess the accuracy of
269 the measurements and were within $6.5 \mu\text{mol kg}^{-1}$ of the reference value. Ischia's temperatures
270 are between 0.87 to 2.67°C higher than in the Bay of Villefranche during the studied period.
271 Water pumped on the Bay of Villefranche was heated to be as close as possible to Ischia's
272 temperatures. Salinity at Ischia and in the Bay of Villefranche-sur-Mer are similar. Salinity
273 data were gathered from the salinity recorded weekly in the Bay of Villefranche by the
274 *Service d'Observation Rade de Villefranche, SO-Rade*, of the *Observatoire Océanologique*
275 *and the Service d'Observation en Milieu Littoral, SOMLIT/CNRS-INSU*. pH_T , temperature, A_T
276 and salinity were used to calculate the other carbonate chemistry parameters using the R
277 package seacarb (Gattuso et al. 2020) (Tab. 1, Tab. S2 Supplementary materials).

278 Six-month and monthly calcification

279 Calcification rate was assessed using the buoyant weight technique (Davies 1989). Weighing
280 was done every 27 to 35 days. Changes in wet weight were converted to dry weight using the
281 following equation:

282
$$dry\ weight = \frac{wet\ weight}{(1 - \frac{water\ density}{aragonite\ density})}$$

283 with an aragonite density of 2.93 g cm³. Six-month calcification rates corresponding to the
284 entire experiment duration were determined as the change in dry weight between the first and
285 the last weighing, normalized by the corals living tissue surface at the end of the experiment
286 and the number of days of the experiment (202 days). Regular rates of calcification over time
287 were normalized to the surface of the corals and to the number of days between weighing
288 (~30 d). Surfaces were determined by the aluminum foil technique for *C. caespitosa* (Marsh
289 1970) because these 3D colonies were impossible to analyze with 2D pictures. *A. calycularis*
290 surfaces were measured by photographic analysis with the software ImageJ for (IMAGEJ,
291 NIH US Department of Health and Human Services) as they had flat shape. Surface
292 measurements were completed at the start and end of the experiment. Marginal changes in
293 surface area were observed between the beginning and end of the experiment.

294 Dark respiration, gross photosynthesis and short-term calcification

295 Dark respiration, net photosynthesis and short-term calcification were determined during less
296 than 1 h incubations in 500 ml transparent perspex chambers, placed in a temperature-
297 controlled water bath to maintain a constant temperature. Incubations were carried out a
298 month after the start of the experiment (hereafter “start”) and a month before the end of the
299 experiment (hereafter “end”) at the same temperature of 20°C. Magnetic stirrers were used to
300 provide water motion in the incubation chambers. Each colony was transferred to an
301 individual chamber filled with water from the experimental tanks from which the corals were
302 taken for the incubation. A blank incubation with no coral colony and filled with water from
303 the same header tank was performed for each four experimental tanks. Incubations lasted 30
304 to 60 min depending on the magnitude of the metabolic activity. To measure oxygen uptake

305 during respiration, colonies were maintained in darkness by covering the chamber with an
306 opaque plastic bag and incubations started after a 10 min acclimation period. Production of
307 oxygen by photosynthesis was only measured on colonies of *C. caespitosa* under an
308 irradiance of $180 \mu\text{mol photons m}^2 \text{ s}^{-1}$. Oxygen saturation within the chambers was measured
309 every 5 s using a fiber optic oxygen sensor (PreSens, OXY-4 mini), which was calibrated at
310 0% saturation in an oxygen-free solution created by saturating seawater with sodium sulfite,
311 and at 100% saturation in an oxygen-saturated seawater obtained by bubbling ambient air
312 during 5 min. The difference in oxygen saturation between the beginning and end of the
313 incubation was converted to $\text{O}_2 \text{ mg L}^{-1}$ using the `gas_O2sat` function of the `marelac R` package
314 (Soetaert et al. 2020). Oxygen consumption was then normalized by coral surface area,
315 incubation time and chamber volume to obtain the rates of respiration (negative in dark
316 conditions) and net photosynthesis (oxygen production in excess of the respiratory demand
317 under light conditions). The rate of gross photosynthesis was calculated by subtracting the
318 respiration rate in dark to the rate of net photosynthesis, with the assumption that respiration
319 rate is the same under light and dark conditions.

320 Water samples were collected at the beginning and end of the incubation for each colony for
321 calcification determination using the alkalinity anomaly technique (Smith and Key 1975).
322 This method relies on the stoichiometric relationship between total alkalinity and
323 calcification, where the precipitation of one mole of CaCO_3 lowers the total alkalinity by two
324 moles. Alkalinity anomalies were normalized by the coral surface area, incubation time, and
325 chamber volume to calculate light and dark calcification rates. The alkalinity anomaly method
326 was only applied to the zooxanthellate *C. caespitosa*.

327

328

329 Data analysis

330 *Biological surveys:* A generalized linear mixed model was used to test for differences in
331 abundance (poisson family) as a function of site (fixed factor, 2 levels) and quadrat as a
332 random effect. Chi-square contingency tables were used to compare the size–frequency
333 distributions between sites. *Laboratory experiment:* The assumptions of normality and
334 equality of variance were evaluated through graphical analyses of residuals using QQ plot
335 functions in R software. Mean values of the colonies in the experimental tank were used as a
336 replicate for six-month calcification. Each incubation was treated as a statistical replica
337 because they were done in individual chambers on single individuals. The effect of header
338 tanks was first tested with an ANOVA and since its significance was negligible ($p > 0.05$), it
339 was not considered in subsequent analyses. A two way-ANOVA was then used to test for
340 differences in net calcification caused by the origin (vent or ambient pH sites) and the pH
341 treatments (present-day or low pH) for both *C. caespitosa* and *A. calycularis*. For net
342 calcification as a function of time, a three-way ANOVA was applied, with origin, pH
343 treatment, and time as fixed factors. Tukey’s post hoc tests were conducted when significant
344 differences were detected. Three-way repeated measure ANOVA was used for dark
345 respiration, gross photosynthesis and short-term calcification since the same colonies of *C.*
346 *caespitosa* and *A. calycularis* were used at the start and end of the incubations. Results have
347 been reported as means \pm standard error of the mean (SE) hereafter, unless otherwise noted.

348 **Results**

349 In situ environmental conditions and populations of corals

350 Water carbonate chemistry and in situ monitoring of seawater pH_T (pH on the total scale) at
351 the CO₂ vent and reference sites with ambient pH showed mean pH_T = 7.91 at Vent 1, pH_T =
352 7.91 at Vent 2, pH_T = 8.05 at Ambient 1, and pH_T = 7.97 at Ambient 2, respectively (Tab. 1).

353 The field surveys showed significant lower abundance of *C. caespitosa* at Vent 1 compared to
354 Ambient 1 (1.8 ± 0.16 colonies versus 3.3 ± 0.35 , $Z = 2.2$, $p < 0.02$, Fig. S3 Supplementary
355 materials). No large colonies of more than 21 cm were found at Vent 1 (Fig. S1,
356 Supplementary materials). This reduction of size was also observed for *A. calycularis* at Vent
357 2 (92 % had up to 10 polyps versus 72 % in Ambient 2), which differed significantly between
358 sites ($\chi^2 = 76.7$, $p < 0.0001$). Abundance of *A. calycularis* was lower in Vent 2 (67.1 ± 10.3 at
359 Vent 2 versus 80.3 ± 14.5 at Ambient 2, $Z = 2.65$, $p < 0.08$).

360

361 **TABLE 1. Measured and estimated seawater physiochemical parameters at the CO₂ vent sites, reference areas with ambient pH and both pH treatment**
362 **in the experimental tanks for salinity (S), temperature (T), total alkalinity (AT), dissolved inorganic carbon (C_T), pH_T, pCO₂, calcite (Ω_c) and aragonite**
363 **(Ω_a) saturation.** Values are means ± SD with 25th and 75th percentiles. Calculated concentrations of C_T, pCO₂, Ω_c and Ω_a are shown. 1: Parameters measured
364 from discrete water samples; 2: parameters measured with in situ sensors. pH conditions: vent system (low pH); ambient pH; ambient pH experimental treatment
365 (present day); acidified pH experimental treatment (low pH).

Local name	pH conditions	S	T (°C)	A _T (μmol kg ⁻¹)	C _T (μmol kg ⁻¹)	pH _T	pCO ₂ (μatm)	Ω _c	Ω _a
Vent1	Low pH	37.9 ¹ ± 0	16.8 ² ± 0.4	2532 ¹ ± 16	2324 ± 47	7.91 ²	626 ± 311	3.69 ± 0.61	2.39 ± 0.39
		(37.9, 37.9), n=3	(16.6, 17.1), n=1326	(2522, 2545), n=25	(2292, 2341), n=1326	(7.89, 7.99), n=1326	(497, 643), n=1326	(3.43, 4.13), n=1326	(2.22, 2.67), n=1326
Ambient 1	Ambient pH	37.3 ¹ ± 0	17.3 ² ± 0.4	2618 ¹ ± 15	2338 ± 20	8.05 ²	448 ± 42	4.80 ± 0.30	3.11 ± 0.19
		(37.2, 37.3), n=3	(17.0, 17.6), n=1331	(2607, 2633), n=14	(2324, 2350), n=1331	(8.03, 8.07), n=1331	(417, 471), n=1331	(4.61, 5.01), n=1331	(2.98, 3.24), n=1331
Vent 2 (Sept 2018)	Low pH	37.3 ¹ ± 0.2	25.9 ² ± 0.2	2564 ¹ ± 7	2542 ± 79	7.65 ²	2905 ± 1664	1.68 ± 0.59	1.11 ± 0.39
		(37.2, 37.5), n=9	(25.8, 26.0), n=1530	(2561, 2566), n=9	(2477, 2585), n=1530	(7.58, 7.90), n=1530	(1724, 3438), n=1530	(1.21, 2.21), n=1530	(0.80, 1.47), n=1530
Vent 2 (June 2019)	Low pH	37.8 ¹ ± 0	21.8 ² ± 2.1	2541 ¹ ± 20	2352 ± 89	7.74 ²	983 ± 868	3.56 ± 1.05	2.33 ± 0.69
		(37.8, 37.8), n=7	(19.8, 23.8), n=1841	(2533, 2550), n=7	(2289, 2389), n=1841	(7.74, 7.93), n=1841	(590, 978), n=1841	(2.96, 4.39), n=1841	(1.94, 2.88), n=1841
Ambient 2	Ambient pH	37.9 ¹ ± 0	26.4 ² ± 1	2642 ¹ ± 17	2324 ± 21	7.97 ²	556 ± 57	5.53 ± 0.32	3.67 ± 0.22
		(37.9, 37.9), n=7	(25.9, 27.0), n=1691	(2629, 2659), n=17	(2310, 2338), n=1691	(7.94, 8.00), n=1691	(513, 597), n=1691	(5.31, 5.75), n=1691	(3.53, 3.82), n=1691
Experimental tanks	Present day	37.8 ± 0.5	22.6 ± 1.9	2542 ± 54	2206 ± 63	8.06 ± 0.06	415 ± 70	5.65 ± 0.69	3.71 ± 0.46
		(37.3, 38.3), n=25	(20.7, 24.5), n=347	(2488, 2596), n=347	(2143, 2269), n=347	(8.00, 8.12), n=347	(345, 485), n=347	(4.96, 6.34), n=347	(3.25, 4.17), n=347
Experimental tanks	Low pH	37.8 ± 0.5	22.7 ± 1.9	2542 ± 54	2389 ± 65	7.73 ± 0.09	1048 ± 237	2.99 ± 0.56	1.97 ± 0.37
		(37.3, 38.3), n=25	(20.8, 24.6), n=348	(2488, 2596), n=348	(2324, 2454), n=348	(7.64, 7.82), n=348	(811, 1285), n=348	(2.43, 3.55), n=348	(1.60, 2.34), n=348

366 Experimental conditions

367 Weekly temperature in the tanks varied according to natural changes in the summer
368 temperature profile at 10 m depth in Ischia, from 19.08 ± 0.06 °C at the end of May 2019
369 (mean \pm SE, n = 24) to 21.51 ± 0.07 °C at the beginning of December (mean \pm SE, n = 24)
370 with a maximum value of 25.17 ± 0.15 °C in August (mean \pm SE, n = 24, Fig. S2
371 Supplementary materials). The “present-day” treatment was maintained at a mean pH_T of 8.06
372 ± 0.06 (n = 347) whereas “low pH” treatment had a pH_T of 7.73 ± 0.09 (n = 348). Salinity was
373 37.8 ± 0.5 (n = 25).

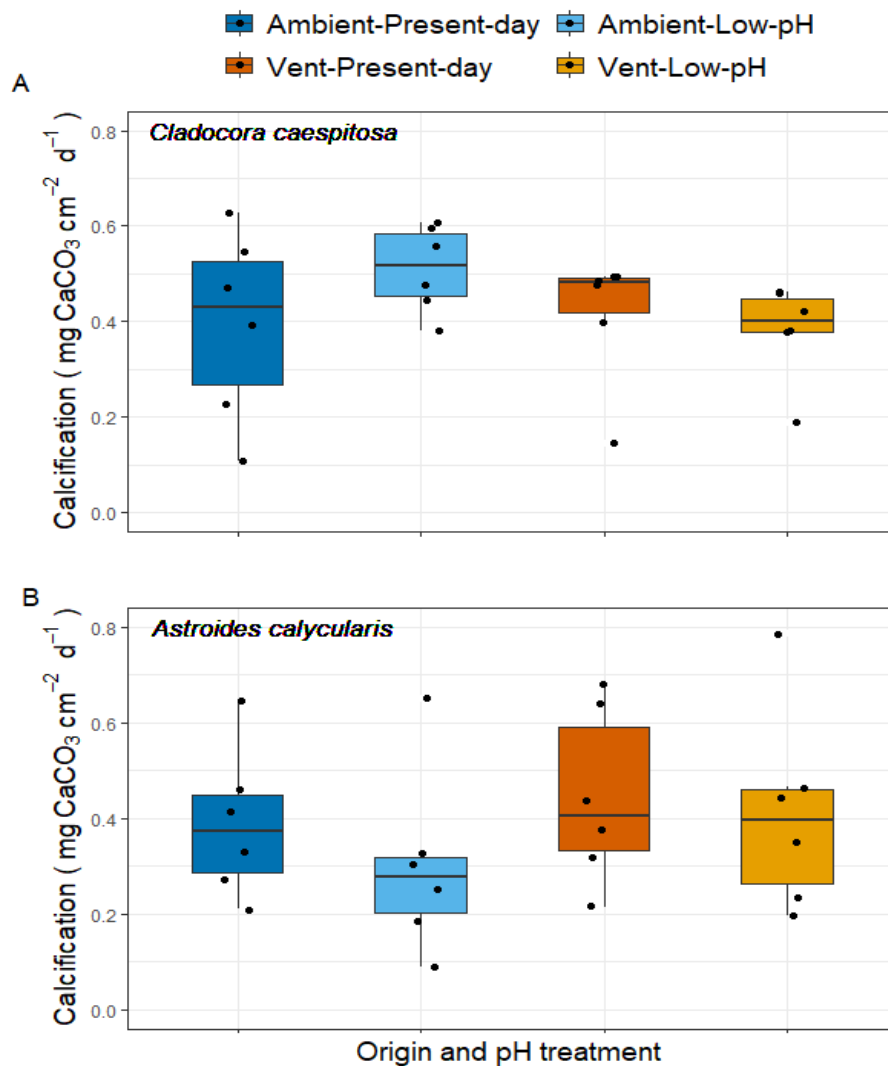
374 Colonies of *Astroides calycularis* had physical differences depending on their site of origin.
375 85% (23/27 colonies) of vent and 14% (2/14 colonies) of ambient colonies did not present
376 coenosarc (i.e. tissue between polyps). Furthermore, by comparing photos from the beginning
377 and end of the experiment, it was observed that none of the *A. calycularis* colonies from
378 ambient suffered polyp death, while three vent colonies showed 2/5, 1/7 and 4/9 dead polyps
379 (number of dead polyps / total number of polyps in the colony). No polyp loss was observed
380 in *Cladocora caespitosa*.

381 Six-month, monthly and short-term calcification rates

382 The rates of six-month calcification of *C. caespitosa* and *A. calycularis* were not affected by
383 the origin and the pH treatment (Fig. 2; Tab. S3 Supplementary materials; Two-way ANOVA,
384 $F_{1,20} = 1.778$, $P = 0.2$ for *C. caespitosa*, $F_{1,20} = 0.13$, $P = 0.72$ for *A. calycularis*).

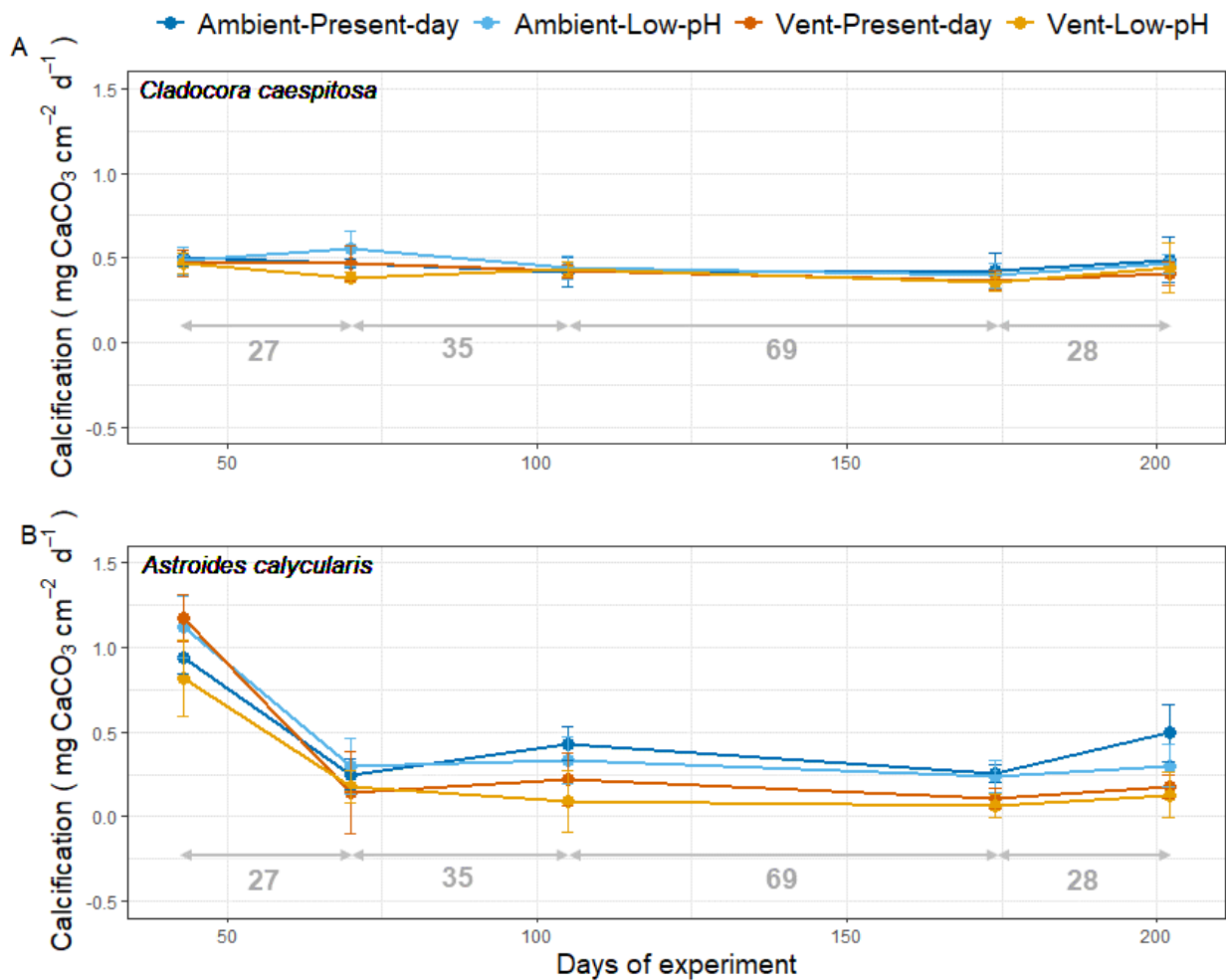
385 No statistically significant effect of origin and pH treatment on calcification rate was found in
386 *C. caespitosa* over time (Fig. 3A; $F_{1,110} = 1.919$, $P = 0.17$). However, different calcification
387 rates with time were found for *A. calycularis* (Fig. 3B, $F_{1,112} = 26.2$, $P < 0.001$), with
388 significantly higher calcification measured during the first month of the experiment (1.0 ± 0.2

389 mg CaCO₃ cm⁻² d⁻¹). The mean monthly calcification rate was 0.2 ± 0.1 mg CaCO₃ cm⁻² d⁻¹
 390 during the following months of experiment.



391

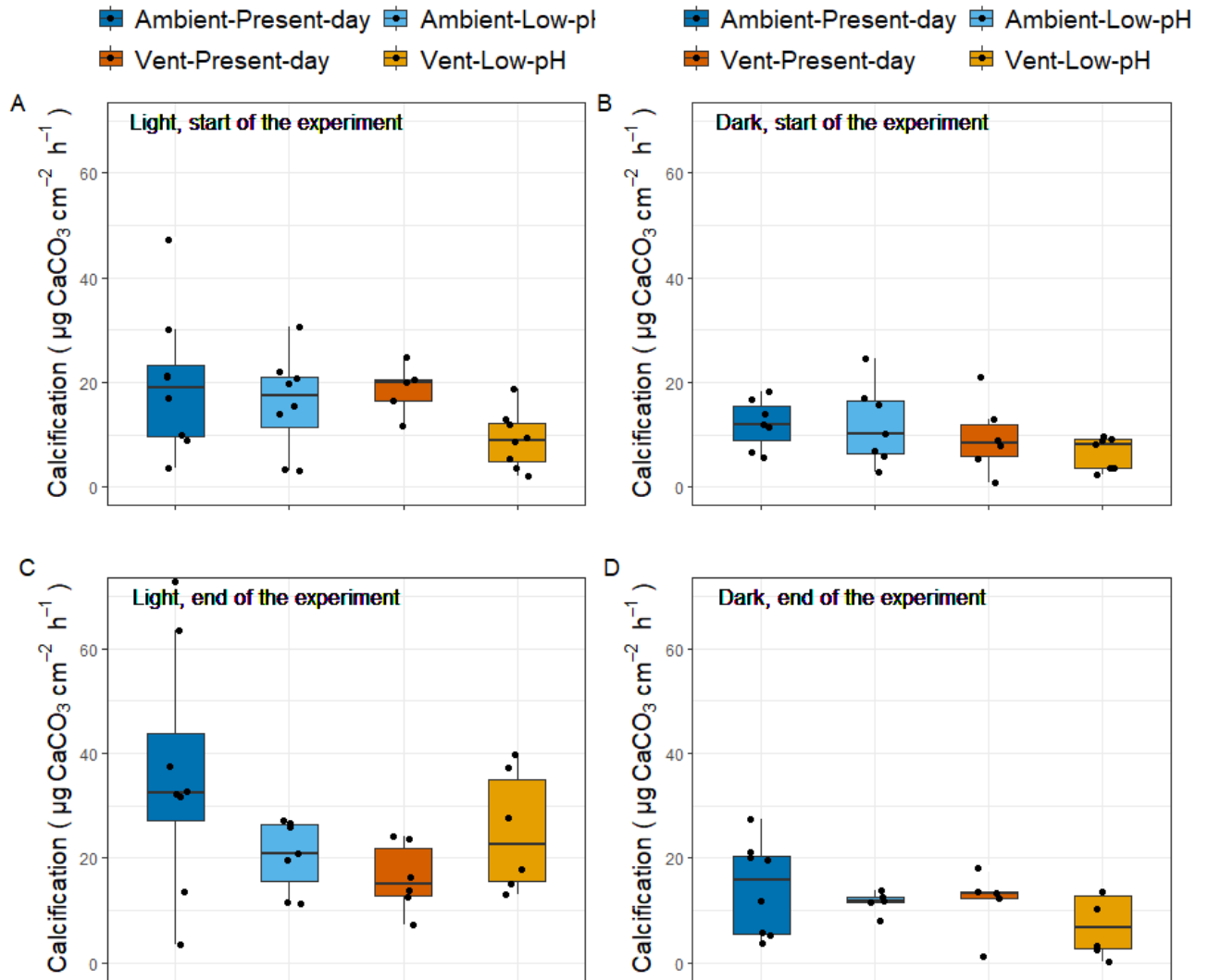
392 **Figure 2. Six-month calcification rates of *C. caespitosa* and *A. calycularis* collected from**
 393 **vent and ambient sites exposed to the two pH treatments (pHT = 8.08 ± 0.01, present**
 394 **day; pHT = 7.72 ± 0.01, low pH) during the entire duration of the experiment (202 days).**
 395 Panel A) shows *Cladocora caespitosa* and panel B) shows *Astroides calycularis*. Dots
 396 represent the mean calcification rates of colonies per experimental tank and boxes represent
 397 the median and the 25 and 75% quartiles. The color of the box indicates the origin and the
 398 treatment. n = 6 per pH treatment and origin.



399

400 **Figure 3. Calcification rates of *C. caespitosa* and *A. calycularis* from vent and ambient**
 401 **sites under the two pH treatments (pH_T = 8.08 ± 0.01, present day; pH_T = 7.72 ± 0.01, low**
 402 **pH) over time (every 27 to 35 days). Values are means ± SE, Panel A) *Cladocora caespitosa***
 403 **and B) *Astroides calycularis*. The color of the dots and lines indicates the origin and the**
 404 **treatment. We had a technical problem with day 139 weighing which is therefore not**
 405 **represented here. Numbers below arrows between dots represent the number of days between**
 406 **measurements. n = 6 per pH treatment and origin.**

407 Short-term calcification of *C. caespitosa* in the dark and in the light was not significantly
 408 different at the start (Fig. 4A and 4B; 10 ± 1.1 and 15.65 ± 1.85 μg CaCO₃ cm⁻² h⁻¹,
 409 respectively) and the end of the experiment (Fig. 4C and 4D; 11.42 ± 1.40 and 25.21 ± 3.03
 410 μg CaCO₃ cm⁻² h⁻¹, respectively). Colonies light and dark calcification were also not affected
 411 by origin and pH treatment (Fig. 4; $F_{1,40} = 0.07$, $P = 0.795$).



412

413 **Figure 4. Short-term calcification rates for *Cladocora caespitosa* from vent and ambient**
 414 **sites under the two pH treatments ($pH_T = 8.08 \pm 0.01$, present day; $pH_T = 7.72 \pm 0.01$, low**
 415 **pH) in the light and dark at the start (27th of June 2019) and end of the experiment (24th**
 416 **of October 2019). Values are means \pm SE. Rates were calculated using alkalinity anomaly**
 417 **method following short term incubations (< 1 h) at 20°C. Panel A) and C) under light**
 418 **conditions, B) and D) under dark conditions. Dots represent the calcification rates of the coral**
 419 **colonies and boxes represent median and 25 and 75% quartiles. The color of the box indicates**
 420 **the origin and the treatment. $n = 5$ to 8 per pH treatment and origin.**

421

422 Dark respiration and gross and net photosynthesis

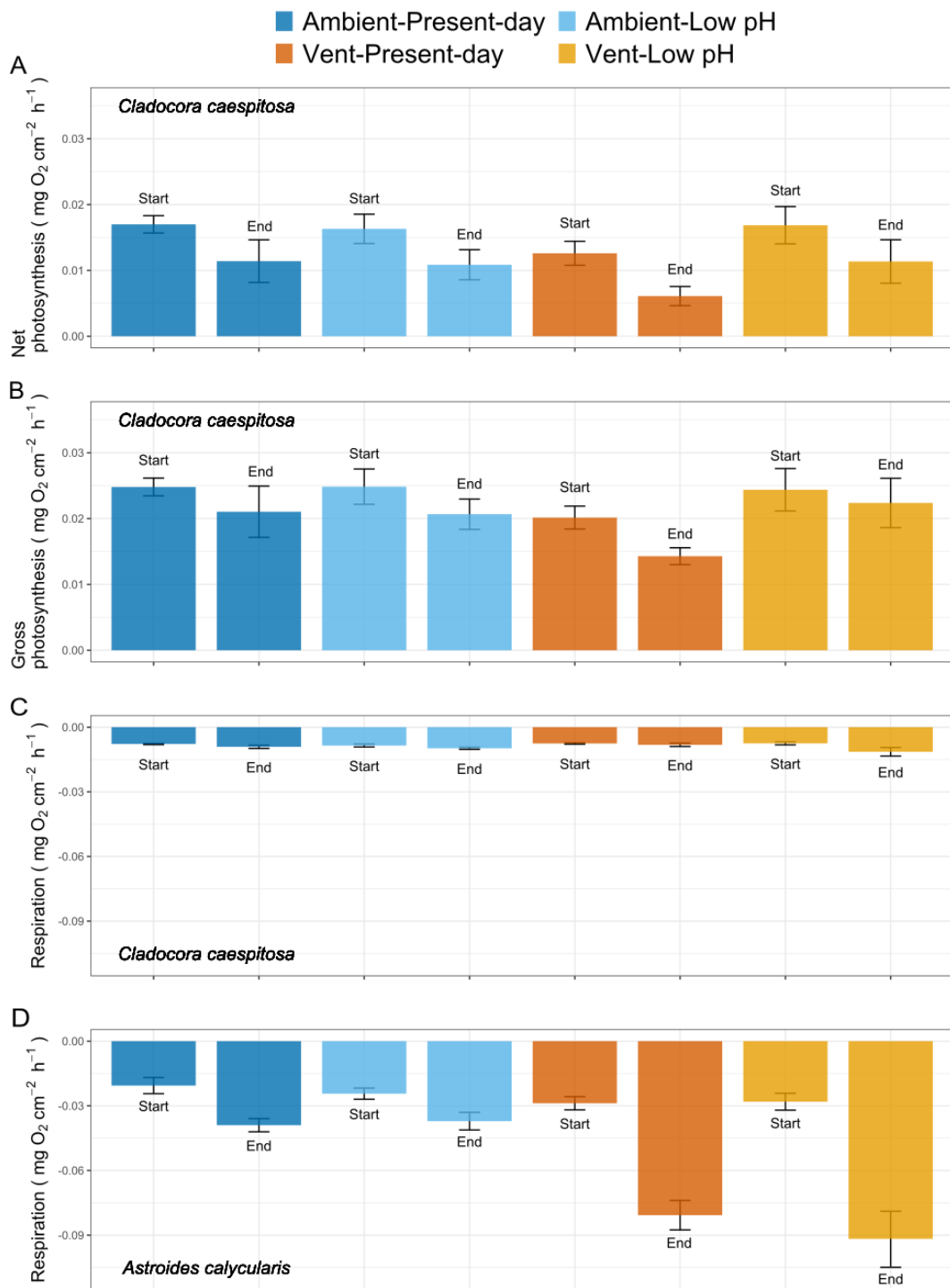
423 Net photosynthesis of *C. caespitosa* was not affected by origin and pH treatment (Fig. 5A;

424 $F_{1,40} = 2.36$, $P = 0.134$ and $F_{1,40} = 1.24$, $P = 0.272$, respectively), but was different between the

425 beginning and the end of the experiment (Fig. 5A; $F_{1,40} = 13.14$, $P < 0.001$). Gross
426 photosynthesis of *C. caespitosa* did not exhibit any statistically significant difference between
427 origin, pH treatment and time (Fig. 5B; $F_{1,24} = 0.17$, $P = 0.683$). Mean gross photosynthesis
428 for all pH treatments was similar at the start and end of the experiment (0.024 ± 0.001 vs
429 0.020 ± 0.002 mg O₂ cm⁻² h⁻¹, n = 30). As light and dark respiration may differ, gross
430 photosynthesis measurements are uncertain, and most likely underestimated.

431 Dark respiration rate of *C. caespitosa* was not significantly different between origin and pH
432 treatment (Fig. 5C, $F_{1,24} = 0.008$, $P = 0.93$ and $F_{1,24} = 3.09$, $P = 0.091$, respectively), but was
433 significantly different between the beginning and end of the experiment ($F_{1,24} = 9.45$, $P =$
434 0.005). In June, mean dark respiration rates for all conditions (origin and pH treatment) was
435 -0.0079 ± 0.0003 mg O₂ cm⁻² h⁻¹ (n = 30) while in November it was -0.0097 ± 0.0006 mg O₂
436 cm⁻² h⁻¹ (n = 28), which represents a 23% of increase in dark respiration.

437 At the start of the experiment, the dark respiration of *A. calycularis* did not differ between
438 origin or pH treatment (Fig. 5D, $F_{1,37} = 0.32$, $P = 0.58$). At the end of the experiment (Fig.
439 5D), a significant difference between site of origin was observed ($F_{1,36} = 18.5$, $P < 0.0001$),
440 with corals from the ambient site having a mean dark respiration of -0.038 ± 0.003 mg O₂ cm⁻²
441 h⁻¹ (n = 13) whilst colonies from the CO₂ vent site had a rate of -0.087 ± 0.008 mg O₂ cm⁻² h⁻¹
442 (n = 27). The overall (all treatments) mean dark respiration rate were also different at the
443 start and at the end of the experiment, with a lower mean dark respiration at the start ($-0.026 \pm$
444 0.002 vs -0.071 ± 0.007 mg O₂ cm⁻² h⁻¹; $F_{1,36} = 52.3$, $P < 0.0001$).



445

446 **Figure 5. Net and gross photosynthesis and dark respiration rates of *C. caespitosa* and *A.***
 447 ***calycularis* from the vent and ambient sites under the two pH treatments (pH_T = 8.08 ±**
 448 **0.01, present day; pH_T = 7.72 ± 0.01, low pH) at the start (27th of June 2019) and end of the**
 449 **experiment (24th of October 2019). Values are means ± SE, Panel A) *Cladocora***
 450 ***caespitosa*'s net photosynthesis, B) *Cladocora caespitosa*'s gross photosynthesis, C)**
 451 ***Cladocora caespitosa*'s dark respiration. D) *Astroides calycularis*' dark respiration. The color**
 452 **of the bars indicates the origin and the treatment. n = 6 to 15 per pH treatment and origin.**

453 **Discussion**

454 During this six-month laboratory experiment, we tested whether colonies of the
455 zooxanthellate coral *Cladocora caespitosa* and the azooxanthellate coral *Astroides calycularis*
456 growing in naturally acidified waters were more tolerant to low pH than colonies from
457 ambient pH sites or acclimated. In contrast to our initial hypothesis, calcification rates and
458 metabolic responses did not change for any coral species no matter the site of origin and pH
459 treatment. Therefore, our results suggest that both species, independently of environmental
460 history and trophic strategy, can tolerate low pH conditions for six months, under controlled
461 conditions in aquaria. In contrast, in situ surveys revealed lower abundance and smaller sizes
462 for both corals at CO₂ vent sites compared with ambient sites.

463 The hypothesis that corals from vent sites would be less impacted by low pH stems from
464 reports that organisms experiencing highly variable or low pH in their natural habitat may be
465 more tolerant to ocean acidification (Cornwall et al. 2018). Corals living in suboptimal
466 environmental conditions may possess physiological and potentially genetic mechanisms that
467 confer tolerance to such environmental conditions (Camp et al 2018, Teixidó et al 2020). For
468 example, microhabitats experiencing periodic temperature extremes are potential habitats for
469 heat tolerant corals (Schoepf et al. 2015), yet these habitats can exhibit a mosaic of
470 populations, harboring species previously reported with high to low thermal tolerance
471 (Ainsworth et al. 2016). Such physiological mechanisms and intraspecific variability may
472 exist in *C. caespitosa* and *A. calycularis* which highlights the importance of studying the
473 influence of suboptimal environmental conditions on tolerance to stressors.

474 Previous research has shown a decrease in calcification when corals were transplanted from
475 ambient pH sites to CO₂ vents (Rodolfo-Metalpa et al. 2011; Prada et al. 2017). However,
476 previous studies on temperate/cold-water coral including *C. caespitosa* and *A. calycularis*
477 have also shown a greater tolerance to ocean acidification than most tropical corals (see Tab.

478 S5 Supplementary materials). Calcification rates reported in the present study agree with
479 earlier studies. For *C. caespitosa*, Rodolfo-Metalpa et al. (2010) observed a yearly
480 calcification rate of $0.51 \text{ mg CaCO}_3 \text{ cm}^{-2} \text{ d}^{-1}$, which is similar to what we measured during
481 this six-month experiment ($0.43 \pm 0.03 \text{ mg CaCO}_3 \text{ cm}^{-2} \text{ d}^{-1}$). The calcification rates of *A.*
482 *calycularis* measured here are also of the same order of magnitude to those reported by
483 Movilla et al. (2016) (0.39 ± 0.04 and $0.47 \pm 0.06 \text{ mg CaCO}_3 \text{ cm}^{-2} \text{ d}^{-1}$, respectively). In
484 contrast to temperate and cold-water corals, tropical corals tend to be more affected by ocean
485 acidification, as they exhibit a mean decrease in calcification of 10-25% when exposed to the
486 pCO_2 expected by the end of the century under the high- CO_2 emissions scenario (Chan and
487 Connolly 2013; Cornwall et al. 2021). Most tropical corals investigated so far are fast
488 calcifiers, growing in warm waters, therefore as seawater pH declines, they may be unable to
489 maintain these energetically costly fast rates of calcification (Comeau et al. 2014). In contrast,
490 temperate and cold-water corals are slower calcifiers with lower energy requirements for
491 mineralization, thus making them more likely to maintain constant calcification rates at lower
492 pH (Rodolfo-Metalpa et al. 2010, Comeau et al. 2014). Ries et al. (2010), also suggested that
493 the effect of acidification on the calcification of temperate corals, such as *Oculina arbuscula*,
494 may manifest at a lower pH threshold compared to tropical corals. The capacity of *C.*
495 *caespitosa* and *A. calycularis* to control the carbonate chemistry at their site of calcification
496 could explain this tolerance to low pH. For example, using the geochemical proxy $\delta^{11}\text{B}$ it was
497 shown that the temperate coral *Balanophyllia europaea* at the CO_2 vents of Panarea Island
498 (Italy) can maintain constant calcifying fluid pH when exposed to pH ranging from 8.07 to
499 7.74 (Wall et al. 2019). This confirms the capacity of some corals to maintain internal pH
500 homeostasis and utilize this as a way of calcifying under reduced seawater pH (Comeau et al.
501 2019).

502 From this study no conclusions can be drawn as to whether colonies from the vent sites are
503 acclimated to low pH, as colonies from both vent sites and the ambient sites were not affected
504 by low pH in the laboratory. However, controlling the transport of calcium and inorganic
505 carbon to the calcifying medium and producing the skeletal organic matrix are all energy-
506 demanding processes (Allemand et al. 2011, Wall et al. 2019), therefore the maintenance of
507 calcification rates under these treatments may have come at a cost. For example, Wall et al.
508 (2019) suggest that the inactivation of some calciblastic cells could compensate for the
509 energy required to regulate internal pH and maintain calcification rates under low seawater
510 pH, but at the cost of increased skeletal porosity. This is supported by a study that showed a
511 constant growth rate of the temperate coral *B. europaea* in acidified conditions at the expense
512 of skeletal density (Fantazzini et al. 2015), which in return increases the sensitivity to
513 bioerosion and susceptibility to damage (Crook et al. 2013). Skeletal porosity was not
514 measured in the present study. However, increased sensitivity to bioerosion can also be linked
515 to the tissue coverage of the skeleton. Rodolfo-Metalpa et al. (2010) observed that following
516 transplantation to low pH conditions, skeleton dissolution was observed in *Cladocora*
517 *caespitosa* which had exposed skeleton, and not in *Balanophyllia europaea* which had less
518 exposed skeleton. In our study, we observed that most of the *A. calycularis* colonies collected
519 at the CO₂ vent sites did not possess coenosarc (i.e. coral tissue between polyps) and exhibited
520 polyp death during our experiment. These phenomena were also observed in natural colonies
521 of *A. calycularis* (Teixidó et al. 2020) and the corals *Pocillopora damicornis* and *Oculina*
522 *patagonica* when incubated at low pH (Kvitt et al. 2015). The increased sensitivity to
523 bioerosion of *A. calycularis* and *C. caespitosa* with exposed skeleton could explain in part the
524 field observation.

525 Field observations confirmed the difference between the population of the CO₂ vent and
526 ambient sites, as both corals were less abundant and had smaller colonies at the vent sites

527 (Fig. S3 Supplementary materials, Teixidó et al. 2020). These contrasting results between
528 field and laboratory observations, could be explained by differences in pH variability, which
529 is much greater in the field with short periods of very low pH. Alternatively, other
530 environmental parameters such as food availability or biological interactions (e.g.,
531 competition with algae) may contribute to these differences. pH variability at the CO₂ vent
532 sites can be very high, as pH_T can range from 6.70 to 8.13 in a day (Foo et al. 2018, Teixidó et
533 al. 2020), whereas pH_T was very stable during our pH-controlled laboratory experiment (pH_T
534 = 7.72 ± 0.01 for low pH treatment). It may be that no differences in calcification and
535 photosynthesis were observed in the laboratory, due to the fact that both corals are slow-
536 growing and long-lived species that have had a lifetime to acclimatize to their environmental
537 pH. Therefore, the six-month time scale of the experiment may not have been enough to
538 trigger any visible variation. However, even if our results did not show any statistical
539 difference between treatments during the laboratory experiment, different trends in
540 calcification between conditions can be observed for *A. calycularis*. The colonies from
541 ambient-low pH condition seem to have lower calcification rate than the control colonies of
542 ambient-present day condition (Fig. 2), suggesting a possible impact of low pH on
543 calcification in the short term. The same trend is observed with the colonies from the vent
544 site, as the vent-low pH presents reduced calcification rate compared to the vent-present day
545 condition. Moreover, calcification was similar in the vent-low pH and the control ambient-
546 present day conditions. This trend suggests a possible acclimation to low pH in corals
547 growing at the CO₂ vent site

548 Zooxanthellate and azooxanthellate corals were both used in the present study to assess the
549 role that photosynthesis could play in mitigating the effects of ocean acidification on
550 calcification. In zooxanthellate corals, light-enhanced calcification describes the relationship
551 between calcification, photosynthesis and irradiance (Gattuso et al. 1999; Allemand et al.

2011). Four main mechanisms explaining light-enhanced calcification were proposed: photosynthesis could (1) supply energy to the animal through the translocation of photosynthates, (2) increase pH at the site of calcification by using CO₂, (3) remove phosphate, which is poison to carbonate crystallization, and (4) facilitate the production of the organic matrix which serves as a scaffold in which CaCO₃ is precipitated (Allemand et al. 2011). Here, short-term calcification of *C. caespitosa* was higher in light than in the dark, with a mean light:dark calcification ratio of 2.38 (See Tab. S4 Supplementary materials), which is close to the mean ratio of 3.0 obtained by Gattuso et al. (1999). However, neither light nor dark calcification rates differed with experimental pH conditions, thus we cannot conclude that photosynthesis did provide better tolerance to ocean acidification. Furthermore, no difference in the response of calcification to ocean acidification was observed between the zooxanthellate (*C. caespitosa*) and azooxanthellate species (*A. calycularis*). The data from the in situ survey at Ischia did not highlight a difference between the zooxanthellate and azooxanthellate corals either, as the size and abundance of colonies from CO₂ vent sites were lower for both species. Contrastingly, Prada et al. (2017) reported that the zooxanthellate coral *B. europaea* was unaffected by low pH conditions, whereas the azooxanthellate corals *Leptosammia pruvoti* and *A. calycularis* showed a negative effect of pH on calcification. However, the study of Prada et al. (2017) was conducted in situ, on corals transplanted next to CO₂ vents in Panarea Island, whereas our study is based on a laboratory experiment and field observations. Feeding could also explain this difference as it can mitigate the negative effects of environmental stressors on coral physiology (Fox et al. 2018). In our experiment, corals were fed freshly hatched *Artemia nauplii* three-times a week therefore the demand of energy required to maintain calcification under low pH was likely sustained by heterotrophy (Edmunds 2011). Kornder et al. (2018) showed that in studies where corals were fed, the negative impacts of ocean acidification on corals were mitigated. Therefore, the fact that

577 Movilla et al. (2012) observed a decrease in calcification at low pH in *C. caespitosa* may be
578 explained by the fact that the colonies were only fed once per week.

579 No difference in photosynthesis was observed between site of origin or pH treatment. This
580 aligns with the observation that there is a limited impact of environmentally relevant
581 decreases in pH on photosynthesis (Comeau et al. 2017), and that low pH rarely causes
582 bleaching (Anthony et al. 2008). Moreover, Mediterranean corals harbor Clade B
583 *Symbiodinium*, that have growth rates, photosynthetic capacities and respiration rates that are
584 unaffected by acidification (Brading et al. 2011). Respiration was also not affected by the pH
585 treatment in *C. caespitosa*, confirming previous observations for this species (Rodolfo-
586 Metalpa et al. 2010), and other coral species (Comeau et al. 2017). However, colonies of *A.*
587 *calycularis* from the vent site exhibited a higher rate of respiration at the end of the
588 experiment (November) for both low and present-day pH treatments. This result contrasts
589 with studies that show a decrease in respiration at lower pH (e.g. Comeau et al. 2014), or no
590 impact on respiration (Rodolfo-Metalpa et al. 2010; Comeau et al. 2017). However, an
591 increase in respiration could be due to the increased energetic demand associated with
592 maintaining calcification rates at lower pH (Comeau et al. 2017). For example, a decrease in
593 seawater pH_T of 0.7 units requires an additional $1-2 \text{ kJ of energy mol}^{-1}$ of CaCO_3
594 precipitated (McCulloch et al. 2012a). For zooxanthellate corals, this energy is less than 1%
595 of the energy provided by photosynthesis, however, for azooxanthellate corals such as *A.*
596 *calycularis*, respiration is the only way to up-regulate this energy demand. Moreover, the
597 increase of respiration from colonies of vent sites of *A. calycularis* could be partly due to the
598 smaller size of colonies at the vent site than at the ambient site (Edmunds and Burgess 2016).

599 Although the corals studied here showed tolerance in the laboratory to pH conditions expected
600 by 2100, it is a fragile equilibrium that can be disrupted by the inclusion of changes in other

601 environmental variables such as temperature that could lead to a greater impact on
602 physiological processes and survival, as observed in the in situ survey and predicted by the
603 negative trend on the calcification of *A. calycularis*. For example, marine heatwaves can lead
604 to mass mortality of *C. caespitosa* and *A. calycularis* (Rodolfo-Metalpa et al. 2005) and are
605 projected to be more frequent and severe in the future (Galli et al. 2017, Smale et al. 2019).
606 Moreover, the impact of ocean acidification on reproduction as well as larval and juvenile
607 survival, which can limit the persistence and dispersion of a species remains to be
608 investigated. The present study contributes to our knowledge of *Cladocora caespitosa* and
609 *Astroides calycularis*' ability to survive under future ocean acidification conditions. Such
610 information will improve our ability to manage and conserve the biodiversity of
611 Mediterranean calcifying species.

612

613

614

615

616

617

618

619

620

621

622

623 **References**

- 624 Ainsworth, T. D., S. F. Heron, J. C. Ortiz, P. J. Mumby, A. Grech, D. Ogawa, C. M. Eakin,
625 and W. Leggat. 2016. Climate change disables coral bleaching protection on the Great
626 Barrier Reef. *Science*. **352**: 338–342. doi:10.1126/science.aac7125
- 627 Allemand, D., É. Tambutté, D. Zoccola, and S. Tambutté. 2011. Coral Calcification, Cells to
628 Reefs, p. 119–150. *In* Z. Dubinsky and N. Stambler [eds.], *Coral Reefs: An Ecosystem in*
629 *Transition*. Springer Netherlands.
- 630 Anthony, K. R. N., D. I. Kline, G. Diaz-Pulido, S. Dove, and O. Hoegh-Guldberg. 2008.
631 Ocean acidification causes bleaching and productivity loss in coral reef builders. *Proc.*
632 *Natl. Acad. Sci.* **105**: 17442–17446. doi:10.1073/pnas.0804478105
- 633 Brading, P., M. E. Warner, P. Davey, D. J. Smith, E. P. Achterberg, and D. J. Suggett. 2011.
634 Differential effects of ocean acidification on growth and photosynthesis among
635 phlotypes of *Symbiodinium* (Dinophyceae). *Limnol. Oceanogr.* **56**: 927–938.
636 doi:10.4319/lo.2011.56.3.0927
- 637 Caldeira, K., and M. E. Wickett. 2003. Anthropogenic carbon and ocean pH. *Nature* **425**:
638 365–365. doi:10.1038/425365a
- 639 Camp, E. F., V. Schoepf, P. J. Mumby, L. A. Hardtke, R. Rodolfo-Metalpa, D. J. Smith, and
640 D. J. Suggett. 2018. The future of coral reefs subject to rapid climate change: lessons
641 from natural extreme environments. *Front. Mar. Sci.* **5**: 1–21.
642 doi:10.3389/fmars.2018.00004
- 643 Chan, N. C. S., and S. R. Connolly. 2013. Sensitivity of coral calcification to ocean
644 acidification: a meta-analysis. *Glob. Chang. Biol.* **19**: 282–290. doi:10.1111/gcb.12011
- 645 Comeau, S., C. E. Cornwall, T. M. DeCarlo, S. S. Doo, R. C. Carpenter, and M. T.

646 McCulloch. 2019. Resistance to ocean acidification in coral reef taxa is not gained by
647 acclimatization. *Nat. Clim. Chang.* **9**: 477–483. doi:10.1038/s41558-019-0486-9

648 Comeau, S., R. C. Carpenter, and P. J. Edmunds. 2017. Effects of $p\text{CO}_2$ on photosynthesis
649 and respiration of tropical scleractinian corals and calcified algae. *ICES J. Mar. Sci.* **74**:
650 1092–1102. doi:10.1093/icesjms/fsv267

651 Comeau, S., P. J. Edmunds, N. B. Spindel, and R. C. Carpenter. 2014. Fast coral reef
652 calcifiers are more sensitive to ocean acidification in short-term laboratory incubations.
653 *Limnol. Oceanogr.* **59**: 1081–1091. doi:10.4319/lo.2014.59.3.1081

654 Cornwall, C. E., S. Comeau, N. A. Kornder, and others. 2021. Global declines in coral reef
655 calcium carbonate production under ocean acidification and warming. *Proc. Natl. Acad.*
656 *Sci.* **118**: e2015265118. doi:10.1073/pnas.2015265118

657 Cornwall, C. E., and others. 2020. A coralline alga gains tolerance to ocean acidification over
658 multiple generations of exposure. *Nat. Clim. Chang.* **10**: 143–146. doi:10.1038/s41558-
659 019-0681-8

660 Cornwall, C. E., S. Comeau, T. M. DeCarlo, B. Moore, Q. D’Alexis, and M. T. McCulloch.
661 2018. Resistance of corals and coralline algae to ocean acidification: Physiological
662 control of calcification under natural pH variability. *Proc. R. Soc. B Biol. Sci.* **285**.
663 doi:10.1098/rspb.2018.1168

664 Crook, E. D., A. L. Cohen, M. Rebolledo-Vieyra, L. Hernandez, and A. Paytan. 2013.
665 Reduced calcification and lack of acclimatization by coral colonies growing in areas of
666 persistent natural acidification. *Proc. Natl. Acad. Sci.* **110**: 11044–11049.
667 doi:10.1073/pnas.1301589110

668 Davies, S. P. 1989. Short-term growth measurements of corals using an accurate buoyant
669 weighing technique. *Mar. Biol.* **101**: 389–395. doi:10.1007/BF00428135

670 Davy, S. K., D. Allemand, and V. M. Weis. 2012. Cell biology of cnidarian-dinoflagellate
671 symbiosis. *Microbiol. Mol. Biol. Rev.* **76**: 229–261. doi:10.1128/MMBR.05014-11

672 Dickson, A. G., C. L. Sabine, and J. R. Christian. 2007. SOP 3a Determination of total
673 alkalinity in sea water using an open-cell titration, p. 191. *In* Guide to best practices for
674 ocean CO₂ measurements. North Pacific Marine Science Organization.

675 Edmunds, P., and R. Gates. 2008. Acclimatization in tropical reef corals. *Mar. Ecol. Prog.*
676 *Ser.* **361**: 307–310. doi:10.3354/meps07556

677 Edmunds, P. J. 2011. Zooplanktivory ameliorates the effects of ocean acidification on the reef
678 coral *Porites* spp. *Limnol. Oceanogr.* **56**: 2402–2410. doi:10.4319/lo.2011.56.6.2402

679 Edmunds, P. J., and S. C. Burgess. 2016. Size-dependent physiological responses of the
680 branching coral *Pocillopora verrucosa* to elevated temperature and *p*CO₂. *J. Exp. Biol.*
681 **219**: 3896–3906. doi:10.1242/jeb.146381

682 Erez, J., S. Reynaud, J. Silverman, K. Schneider, and D. Allemand. 2011. Coral calcification
683 under ocean acidification and global change, p. 151–176. *In* Z. Dubinsky and N.
684 Stambler [eds.], *Coral Reefs: An Ecosystem in Transition*. Springer Netherlands.

685 Fabricius, K. E., and others. 2011. Losers and winners in coral reefs acclimatized to elevated
686 carbon dioxide concentrations. *Nat. Clim. Chang.* **1**: 165–169. doi:10.1038/nclimate1122

687 Fantazzini, P., and others. 2015. Gains and losses of coral skeletal porosity changes with
688 ocean acidification acclimation. *Nat. Commun.* **6**: 7785. doi:10.1038/ncomms8785

689 Foo, S. A., M. Byrne, E. Ricevuto, and M. C. Gambi. 2018. The carbon dioxide vents of
690 Ischia, Italy, a natural system to assess impacts of ocean acidification on marine
691 ecosystems: an overview of research and comparisons with other vent systems, p. 237–
692 310. *In* S.J. Hawkins, A.J. Evans, A.C. Dale, L.B. Firth, and I.P. Smith [eds.],

693 Oceanography and Marine Biology. CRC Press.

694 Foster, T., and P. L. Clode. 2016. Skeletal mineralogy of coral recruits under high temperature
695 and $p\text{CO}_2$. *Biogeosciences* **13**: 1717–1722. doi:10.5194/bg-13-1717-2016

696 Fox, M. D., and others. 2018. Gradients in primary production predict trophic strategies of
697 mixotrophic corals across spatial scales. *Curr. Biol.* **28**: 3355-3363.e4.
698 doi:10.1016/j.cub.2018.08.057

699 Galli, G., C. Solidoro, and T. Lovato. 2017. Marine heat waves hazard 3D maps and the risk
700 for low motility organisms in a warming Mediterranean Sea. *Front. Mar. Sci.* **4**: 1–14.
701 doi:10.3389/fmars.2017.00136

702 Gattuso, J.-P., D. Allemand, and M. Frankignoulle. 1999. Photosynthesis and calcification at
703 cellular, organismal and community levels in coral reefs: A review on interactions and
704 control by carbonate chemistry. *Am. Zool.* **39**: 160–183. doi:10.1093/icb/39.1.160

705 Gattuso, J. -P., J.-M. Epitalon, H. Lavigne, and J. C. Orr. 2020. seacarb: seawater carbonate
706 chemistry. R package version 3.2.13. <https://cran.r-project.org/package=seacarb>.

707 Gibbin, E. M., H. M. Putnam, S. K. Davy, and R. D. Gates. 2014. Intracellular pH and its
708 response to CO_2 -driven seawater acidification in symbiotic versus non-symbiotic coral
709 cells. *J. Exp. Biol.* **217**: 1963–1969. doi:10.1242/jeb.099549

710 González-Delgado, S., and J. C. Hernández. 2018. The importance of natural acidified
711 systems in the study of ocean acidification: what have we learned?, p. 57–99. *In*
712 *Advances in Marine Biology*. Academic Press.

713 Gruber, N., and others. 2019. The oceanic sink for anthropogenic CO_2 from 1994 to 2007.
714 *Science* (80-.). **363**: 1193–1199. doi:10.1126/science.aau5153

715 Hall-Spencer, J. M., and others. 2008. Volcanic carbon dioxide vents show ecosystem effects

716 of ocean acidification. *Nature* **454**: 96–99. doi:10.1038/nature07051

717 Inoue, M., T. Nakamura, Y. Tanaka, A. Suzuki, Y. Yokoyama, H. Kawahata, K. Sakai, and N.
718 Gussone. 2018. A simple role of coral-algal symbiosis in coral calcification based on
719 multiple geochemical tracers. *Geochim. Cosmochim. Acta* **235**: 76–88.
720 doi:10.1016/j.gca.2018.05.016

721 Kersting, D.-K., and C. Linares. 2012. *Cladocora caespitosa* bioconstructions in the
722 Columbretes Islands Marine Reserve (Spain, NW Mediterranean): distribution, size
723 structure and growth. *Mar. Ecol.* **33**: 427–436. doi:10.1111/j.1439-0485.2011.00508.x

724 Kornder, N. A., B. M. Riegl, and J. Figueiredo. 2018. Thresholds and drivers of coral
725 calcification responses to climate change. *Glob. Chang. Biol.* **24**: 5084–5095.
726 doi:10.1111/gcb.14431

727 Kroeker, K. J., R. L. Kordas, R. Crim, I. E. Hendriks, L. Ramajo, G. S. Singh, C. M. Duarte,
728 and J.-P. Gattuso. 2013a. Impacts of ocean acidification on marine organisms:
729 quantifying sensitivities and interaction with warming. *Glob. Chang. Biol.* **19**: 1884–
730 1896. doi:10.1111/gcb.12179

731 Kroeker, K. J., M. C. Gambi, and F. Micheli. 2013b. Community dynamics and ecosystem
732 simplification in a high-CO₂ ocean. *Proc. Natl. Acad. Sci.* **110**: 12721–12726.
733 doi:10.1073/pnas.1216464110

734 Kvitt, H., E. Kramarsky-Winter, K. Maor-Landaw, K. Zandbank, A. Kushmaro, H. Rosenfeld,
735 M. Fine, and D. Tchernov. 2015. Breakdown of coral colonial form under reduced pH
736 conditions is initiated in polyps and mediated through apoptosis. *Proc. Natl. Acad. Sci.*
737 U. S. A. **112**: 2082–2086. doi:10.1073/pnas.1419621112

738 Linares, C., and others. 2015. Persistent natural acidification drives major distribution shifts in

739 marine benthic ecosystems. *Proc. R. Soc. B Biol. Sci.* **282**: 20150587.
740 doi:10.1098/rspb.2015.0587

741 Marsh, J. A. J. 1970. Primary productivity of reef-building calcareous red algae. *Ecol. Soc.*
742 *Am.* **51**: 255–263.

743 Martin, S., and J.-P. Gattuso. 2009. Response of Mediterranean coralline algae to ocean
744 acidification and elevated temperature. *Glob. Chang. Biol.* **15**: 2089–2100.
745 doi:10.1111/j.1365-2486.2009.01874.x

746 McCulloch, M., J. Falter, J. Trotter, and P. Montagna. 2012a. Coral resilience to ocean
747 acidification and global warming through pH up-regulation. *Nat. Clim. Chang.* **2**: 623–
748 627. doi:10.1038/nclimate1473

749 McCulloch, M., and others. 2012b. Resilience of cold-water scleractinian corals to ocean
750 acidification: Boron isotopic systematics of pH and saturation state up-regulation.
751 *Geochim. Cosmochim. Acta* **87**: 21–34. doi:10.1016/j.gca.2012.03.027

752 Movilla, J., E. Calvo, R. Coma, E. Serrano, À. López-Sanz, and C. Pelejero. 2016. Annual
753 response of two Mediterranean azooxanthellate temperate corals to low-pH and high-
754 temperature conditions. *Mar. Biol.* **163**: 135. doi:10.1007/s00227-016-2908-9

755 Movilla, J., E. Calvo, C. Pelejero, R. Coma, E. Serrano, P. Fernández-Vallejo, and M. Ribes.
756 2012. Calcification reduction and recovery in native and non-native Mediterranean corals
757 in response to ocean acidification. *J. Exp. Mar. Bio. Ecol.* **438**: 144–153.
758 doi:10.1016/j.jembe.2012.09.014

759 Muller-Parker, G., C. F. D’Elia, and C. B. Cook. 2015. Interactions between corals and their
760 symbiotic algae. *Coral Reefs Anthr.* 99–116. doi:10.1007/978-94-017-7249-5_5

761 Ohki, S., and others. 2013. Calcification responses of symbiotic and aposymbiotic corals to

762 near-future levels of ocean acidification. *Biogeosciences* **10**: 6807–6814.
763 doi:10.5194/bg-10-6807-2013

764 Orr, J. C., and others. 2005. Anthropogenic ocean acidification over the twenty-first century
765 and its impact on calcifying organisms. *Nature* **437**: 681–686. doi:10.1038/nature04095

766 Peirano, A., C. Morri, C. N. Bianchi, and R. Rodolfo-Metalpa. 2001. Biomass, carbonate
767 standing stock and production of the mediterranean coral *Cladocora caespitosa* (L.).
768 *Facies* **44**: 75–80. doi:10.1007/BF02668168

769 Prada, F., and others. 2017. Ocean warming and acidification synergistically increase coral
770 mortality. *Sci. Rep.* **7**: 1–10. doi:10.1038/srep40842

771 Ries, J. B., A. L. Cohen, and D. C. McCorkle. 2010. A nonlinear calcification response to
772 CO₂-induced ocean acidification by the coral *Oculina arbuscula*. *Coral Reefs* **29**: 661–
773 674. doi:10.1007/s00338-010-0632-3

774 Rodolfo-Metalpa, R., and others. 2011. Coral and mollusc resistance to ocean acidification
775 adversely affected by warming. *Nat. Clim. Chang.* **1**: 308–312.
776 doi:10.1038/nclimate1200

777 Rodolfo-Metalpa, R., S. Martin, C. Ferrier-Pagès, and J. P. Gattuso. 2010. Response of the
778 temperate coral *Cladocora caespitosa* to mid- and long-term exposure to *p*CO₂ and
779 temperature levels projected for the year 2100 AD. *Biogeosciences* **7**: 289–300.
780 doi:10.5194/bg-7-289-2010

781 Rodolfo-Metalpa, R., C. N. Bianchi, A. Peirano, and C. Morri. 2005. Tissue necrosis and
782 mortality of the temperate coral *Cladocora caespitosa*. *Ital. J. Zool.* **72**: 271–276.
783 doi:10.1080/11250000509356685

784 Savolainen, O., M. Lascoux, and J. Merilä. 2013. Ecological genomics of local adaptation.

785 Nat. Rev. Genet. **14**: 807–820. doi:10.1038/nrg3522

786 Schoepf, V., M. Stat, J. L. Falter, and M. T. McCulloch. 2015. Limits to the thermal tolerance
787 of corals adapted to a highly fluctuating, naturally extreme temperature environment.
788 Sci. Rep. **5**: 17639. doi:10.1038/srep17639

789 Smale, D. A., and others. 2019. Marine heatwaves threaten global biodiversity and the
790 provision of ecosystem services. Nat. Clim. Chang. **9**: 306–312. doi:10.1038/s41558-
791 019-0412-1

792 Smith, S. V., and G. S. Key. 1975. Carbon dioxide and metabolism in marine environments.
793 Limnol. Oceanogr. **20**: 493–495.

794 Soetaert, K., T. Petzoldt, F. Meysman, and L. Meire. 2020. marelac : Tools for aquatic
795 sciences. R package version 2.1.10. <https://cran.r-project.org/package=marelac>.

796 Teixidó, N., M. C. Gambi, V. Parravacini, K. Kroeker, F. Micheli, S. Villéger, and E.
797 Ballesteros. 2018. Functional biodiversity loss along natural CO₂ gradients. Nat.
798 Commun. **9**: 1–9. doi:10.1038/s41467-018-07592-1

799 Teixidó, N., and others. 2020. Ocean acidification causes variable trait-shifts in a coral
800 species. Glob. Chang. Biol. **26**: 6813–6830. doi:10.1111/gcb.15372

801 Trotter, J., and others. 2011. Quantifying the pH “vital effect” in the temperate zooxanthellate
802 coral *Cladocora caespitosa*: Validation of the boron seawater pH proxy. Earth Planet.
803 Sci. Lett. **303**: 163–173. doi:10.1016/j.epsl.2011.01.030

804 Varnerin, B., B. Hopkinson, and D. Gleason. 2020. Recruits of the temperate coral *Oculina*
805 *arbuscula* mimic adults in their resilience to ocean acidification. Mar. Ecol. Prog. Ser.
806 **636**: 63–75. doi:10.3354/meps13228

807 Wall, M., and others. 2019. Linking internal carbonate chemistry regulation and calcification

808 in corals growing at a Mediterranean CO₂ vent. *Front. Mar. Sci.* **6**: 1–12.

809 doi:10.3389/fmars.2019.00699

810 Wang, C., E. M. Arneson, D. F. Gleason, and B. M. Hopkinson. 2020. Resilience of the
811 temperate coral *Oculina arbuscula* to ocean acidification extends to the physiological
812 level. *Coral Reefs*. doi:10.1007/s00338-020-02029-y

813 Zibrowius, H. 1995. The “Southern” *Astroides calycularis* in the Pleistocene of the northern
814 Mediterranean—An indicator of climatic changes (Cnidaria, scleractinia). *Geobios* **28**:
815 9–16. doi:10.1016/S0016-6995(95)80201-0

816

817 **Acknowledgements**

818 This research was supported by the French Government through the National Research
819 Agency - Investments for the Future (“4Oceans-Make Our Planet Great Again” grant, ANR-
820 17-MPGA-0001). Thanks are due to the *Service d’Observation Rade de Villefranche* (SO-
821 Rade) of the *Institut de la mer de Villefranche* and the *Service d’Observation en Milieu*
822 *Littoral* (SOMLIT/CNRS-INSU) for their kind permission to use the Point B data. We thank
823 Samir Alliouane for assistance in the laboratory and P. Sorvino (ANS Diving, Ischia) for
824 assistance in the field.

825 **Author contributions**

826 S.C., N.T., B.M., and J.-P.G designed the study. N.T., S.C., A.M. and B.M. were involved with
827 fieldwork. C.C, B.M., T.G., S.C., and N.T performed the experiments. C.C., N.T. and A.M.
828 analyzed the data. C.C. wrote the first draft of the manuscript which was then finalized by all
829 co-authors.